Archives of Biochemistry and Biophysics 503 (2010) 161–174

Contents lists available at ScienceDirect

Archives of Biochemistry and Biophysics

journal homepage: www.elsevier.com/locate/yabbi

Review

Molecular enzymology of lipoxygenases

Igor Ivanov [a], Dagmar Heydeck [a], Katharina Hofheinz [a], Jana Roffeis [a], Valerie B. O'Donnell [b], Hartmut Kuhn [a,*], Matthias Walther [a]

[a] Institute of Biochemistry, University Medicine Berlin – Charité, Oudenarder Str. 16, D-13347 Berlin, Germany
[b] School of Medicine, Heath Park, Cardiff University, CF14 4XN, UK

ARTICLE INFO

Article history:
Received 16 July 2010
and in revised form 19 August 2010
Available online 27 August 2010

Keywords:
Eicosanoids
Lipid peroxidation
Inflammation
Cell development
Catalysis
Knockout mice
Radicals

ABSTRACT

Lipoxygenases (LOXs) are lipid peroxidizing enzymes, implicated in the pathogenesis of inflammatory and hyperproliferative diseases, which represent potential targets for pharmacological intervention. Although soybean LOX1 was discovered more than 60 years ago, the structural biology of these enzymes was not studied until the mid 1990s. In 1993 the first crystal structure for a plant LOX was solved and following this protein biochemistry and molecular enzymology became major fields in LOX research. This review focuses on recent developments in molecular enzymology of LOXs and summarizes our current understanding of the structural basis of LOX catalysis. Various hypotheses explaining the reaction specificity of different isoforms are critically reviewed and their pros and cons briefly discussed. Moreover, we summarize the current knowledge of LOX evolution by profiling the existence of LOX-related genomic sequences in the three kingdoms of life. Such sequences are found in eukaryotes and bacteria but not in archaea. Although the biological role of LOXs in lower organisms is far from clear, sequence data suggests that this enzyme family might have evolved shortly after the appearance of atmospheric oxygen on earth.

Introduction

Lipoxygenases (LOXs)[1] are non-heme iron-containing dioxygenases [1–3] that catalyze the stereo-specific peroxidation of polyunsaturated fatty acids containing at least one 1-cis,4-cis-pentadiene system (Fig. 1). Fatty acid oxygenation by LOXs generally consists of four elementary reactions (hydrogen abstraction, radical rearrangement, oxygen insertion, peroxy radical reduction), usually proceeding in a sterically controlled manner (Fig. 1). Hydrogen abstraction, which constitutes the rate limiting step [4], follows a quantum-mechanical mechanism [5]. In soybean LOX1, H-atom transfer corresponds to a proton-coupled electron transfer [6,7]. The transferred electron does not localize on the proton, but tunnels directly from the substrate to the ferric iron in a concerted proton tunneling–electron tunneling process [6]. In the transition state the covalently linked Fe–O–H–C bridge lowers the energy barrier and provides an efficient pathway for this tunneling [6].

In most cells, the concentration of free fatty acids is limited and thus, LOX substrates have to be liberated from cellular stores by ester lipid hydrolyzing enzymes [8]. However, certain LOX-isoforms are capable of oxygenating polyunsaturated fatty acids that are incorporated in ester lipids located in biomembranes or lipoproteins [9–11]. The conventional nomenclature classifies animal LOXs with respect to their positional specificity of arachidonic acid oxygenation as 5-LOXs, 8-LOXs, 11-LOXs, 12-LOXs or 15-LOXs. This classification is not optimum since: (i) Arachidonic acid is not a good substrate for many non-mammalian LOXs and with other substrate fatty acids (e.g. linoleic acid) their reaction specificity can be quite different. (ii) Evolutionarily-related LOX-isoforms can exhibit distinct reaction specificities in contrast to those sharing a low degree of phylogenetic relatedness. Moreover, the rapidly growing availability of genomic sequences and our inability to predict the reaction specificity of arachidonic acid oxygenation from the primary structure of the enzymes leads to the confusing situation that most LOX-isoforms (for which we only have sequence information) cannot be classified according to a function-based enzyme nomenclature. Thus, a sequence-based classification procedure that considers the phylogenetic relatedness of the enzymes is desirable. Unfortunately, despite numerous attempts, no simple and unifying LOX nomenclature has been introduced that overcomes the above mentioned problems. The lack of comprehensive and straightforward classification criteria makes it difficult for non-expert scientists to follow the current developments in LOX research.

* Corresponding author. Fax: +49 30 450 528905.
E-mail address: hartmut.kuehn@charite.de (H. Kuhn).

[1] *Abbreviation used:* LOX(s), lipoxygenase(s); 15-H(p)ETE, (5Z,8Z,11Z,13E)-15-hydro(pero)xyeicosa-5,8,11,13-tetraenoic acid; 12-H(p)ETE, (5Z,8Z,10E,14Z)-12-hydro(pero)xyeicosa-5,8,10,14-tetraenoic acid; 11-H(p)ETE, (5Z,8Z,12E,14Z)-11-hydro(pero)xyeicosa-5,8,12,14-tetraenoic acid; 8-H(p)ETE, (5Z,9E,11Z,14Z)-8-hydro(pero)xyeicosa-5,9,11,14-tetraenoic acid; 5-H(p)ETE, (6E,8Z,11Z,14Z)-5-hydro(pero)xyeicosa-6,8,11,14-tetraenoic acid; 13-H(p)ODE, (9Z,11E)-13-hydro(pero)xyoctadeca-9,11-dienoic acid; SAXS, small angle X-ray scattering.

0003-9861/$ - see front matter © 2010 Elsevier Inc. All rights reserved.
doi:10.1016/j.abb.2010.08.016

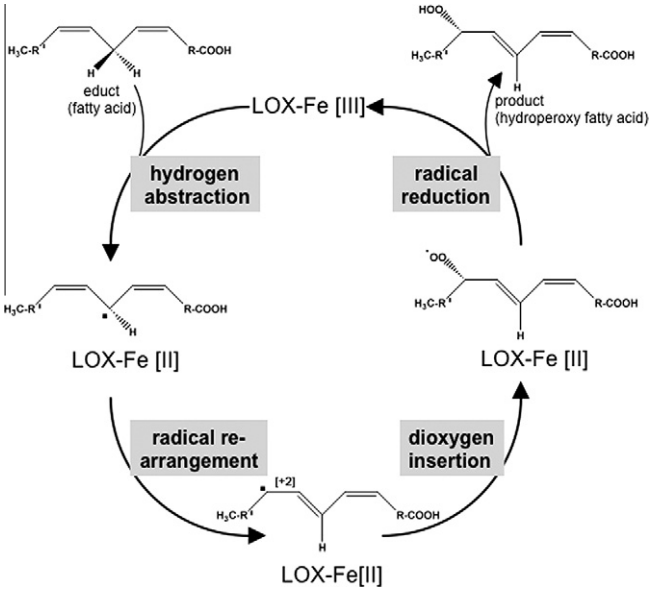

Fig. 1. Detailed mechanism of the LOX-reaction. LOX catalyzed oxygenation of fatty acids consists of four consecutive elementary reactions, the stereochemistry of which are tightly controlled. (i) Stereoselective hydrogen abstraction from a bisallylic methylene: The hydrogen atom is removed as proton and the resulting electron is picked up by the ferric non-heme iron that is reduced to the ferrous form. (ii) Radical rearrangement: During this elementary reaction the radical electron is dislocated either in the direction of the methyl end of the fatty acid ([+2] rearrangement) or in the direction of the carboxylate ([−2] rearrangement). (iii) Oxygen insertion: Molecular dioxygen is introduced antarafacially (from opposite direction of the plane determined by the double bond system) related to hydrogen abstraction. If the hydrogen located above the double bond plane is removed, dioxygen is introduced from below this plane. (iv) peroxy radical reduction: The peroxy radical formed via oxygen insertion is reduced by an electron from the ferrous non-heme iron converting the radical to the corresponding anion. Thereby the iron is reoxidized to its ferric form. Finally, the peroxy anion is protonated.

Another confusing problem, which LOX research shares with other areas in molecular enzymology, is isoform-multiplicity within a particular species and functional heterogeneity of the different isoenzymes. In soybeans, up to 13 different LOX-isoforms have been identified, while the rice genome contains more than 20 different LOX genes. The human genome contains six functional LOX genes, five of which are found clustered on chromosome 17 with only the 5-LOX gene on chromosome 10. In contrast, the murine genome contains seven functional LOX genes (the gene for the murine epidermis 12S-LOX is a functionless pseudogene in the human LOX gene cluster), located in a syntenic region on the mouse chromosome 11. Here again, only 5-LOX is located on a different chromosome (chromosome 6).

A Pubmed search with the keyword "lipoxygenase" gives about 14,000 hits with more than 500 new articles published annually. Thus, it is impossible to reference all of these papers in our review. Furthermore, this article is intended to cover thematic priorities, which have either emerged recently or have not been reviewed in the past. Since we will focus on structural and evolutionary aspects, a detailed discussion of the biological function of LOXs goes beyond the scope of this review. However, we wish to point out two aspects of LOX biology: (i) 30 years ago leukotrienes generated by 5-LOX were identified as potent pro-inflammatory mediators [12] [13]. Since then, additional pro-inflammatory products have been discovered [14]. On the other hand, anti-inflammatory and/or pro-resolving lipids generated by mammalian isoforms have also been identified, including lipoxins [15,16], resolvins [17], protectins [18,19] and maresins [20]. Thus, LOX products play important roles in the development of acute inflammation but they have also been implicated in inflammatory resolution. (ii) Mice deficient in 12R-LOX develop normally during pregnancy but die immediately after birth due to excessive dehydration [21,22]. Although the molecular mechanisms of postpartum mortality are unknown, the enzyme was implicated in the formation of the epidermal water barrier. Genetic polymorphisms of the corresponding human gene have been related to ichthyosis [23], a disease characterized by dry, thickened, scaly or flaky skin.

To obtain more information on different aspects of LOX biology the reader is referred to other reviews, which address their role in cancer [24–26], vascular biology [27,28], and inflammation [29,30].

The structural basis of LOX catalysis

Mammalian lipoxygenases consist of a single polypetide chain that folds into a two-domain structure but in lower organisms fusion proteins may occur

The complete crystal structures of several plant and animal LOXs are available (Table 1), along with a partial set of X-ray coordinates for the human platelet-type 12-LOX. X-ray data is also available for enzyme–ligand complexes of plant LOXs (Table 1).

Most LOXs consist of a single polypeptide chain that folds into a two-domain structure; a small N-terminal β-barrel domain and a larger mostly helical catalytic domain. The rabbit 12/15-LOX (Fig. 2A) is of cylindric shape (height of 10 nm) with an eliptic ground square (longer diameter 6.1 nm, shorter one of 4.5 nm). The structure of coral 8R-LOX (Fig. 2B) is closely related to the rabbit enzyme also resembling a cylinder (diameter 6 nm, height 10 nm) [48]. In contrast, the soybean LOX1 (Fig. 2C) is ellipsoid (9 nm × 6.5 nm × 6 nm) [36].

In lower organisms, LOXs may occur as fusion proteins, in which the LOX-domain is linked to another catalytic domain that plays a role in the secondary metabolism of hydroperoxy fatty acids. The first LOX-fusion protein was discovered in the coral *Plexaura homomalla* [50]. Here, the LOX-domain that produces 8R-HpETE is linked to a heme-containing peroxidase domain, which converts the fatty acid peroxide to an allene oxide. This unstable intermediate may further be converted to cyclopentenone eicosanoids. The fusion protein was cloned and the two subenzymes were separately expressed and characterized [51,52]. Their crystal structures were also solved [34,48,53]. Although the degree of amino acid conservation between the LOX-domain of this fusion protein and the rabbit 12/15-LOX was not particularly impressive (30%), the 3D-structures of the two LOX-isoforms are rather similar. The low-resolution structure of the whole fusion protein indicated that the allene oxide synthase domain interacts non-covalently with both LOX sub-domains while the putative calcium-binding sites and the membrane interacting Trp residues (see "The small N-terminal LOX-domain is important for membrane binding and regulates the catalytic activity") are not shielded but remain surface exposed [49]. Membrane binding of the fusion protein induces alterations in the spatial orientation of the different sub-domains (interdomain movement), as indicated by the appearance of a new proteolytic cleavage site [49].

Another LOX-fusion protein, sharing 84% sequence identity with the *P. homomalla* enzyme, was detected in the coral *Gersemia fruticosa* [54] suggesting a broader distribution of these enzymes in octocorals. In addition, allene oxide synthase/LOX-fusion proteins have been discovered in the cyanobacteria *Anabaena PCC 7120* and *Acaryochloris marina* [55,56]. In contrast to the coral enzymes, in which the fusion proteins contain complete LOXs, the cyanobacteria isoforms lack the N-terminal LOX-domain and the catalytic LOX-domain is truncated (but active). Although the biological role of these fusion proteins is unclear, they have been implicated in the biosynthesis of lipid signaling molecules [50,57]. In all LOX-fu-

Table 1
Structural data available for LOXs from the protein data bank. In addition to the given LOX structures some mutants of soybean LOX1 [31–33] and of coral 8R-LOX [34] have been published. Furthermore, homology based models of the structures of human 15-LOX1 (2ABT), 12-LOX (2ABU), and 5-LOX (2ABV) were released by A. Prakasam and P. Mathur (to be published). The best resolved structure of each isoform is given in bold.

LOX-isoform	Remarks/ligands	Resolution	PDB entry	Reference
Soybean LOX1		2.60	2SBL	[35]
		1.40	1YGE	[36]
	New refinement of 1YGE	1.40	**1F8N**	[32]
Soybean LOX3		2.60	1LNH	[37]
	At ambient temperature	2.0	1RRH	[38]
	at 93 K	2.0	**1RRL**	[38]
Soybean VLX-B		2.4	**2IUJ**	[39]
Soybean VLX-D		2.4	**2IUK**	[39]
Soybean LOX3	With 4-hydroperoxy-2-methoxy-phenol	2.2	1HU9	[40]
Soybean LOX3	With 13S-HPODE	2.0	1IK3	[41]
Soybean LOX3	With protocatechuic acid	2.1	1N8Q	[42]
Soybean LOX3	With epigallocatechin	2.1	1JNQ	[43]
Soybean LOX3	With 4-nitrocatechol	2.15	1NO3	[44]
			(1BYT)	[45]
Rabbit 12/15-LOX	With inhibitor RS7	2.40	1LOX	[46]
	New refinement of 1LOX, dimer with and without inhibitor RS7	2.40	**2P0M**	[47]
Coral 8R-LOX		3.2	2FNQ	[48]
		1.85	**3FG1**	[34]
Plexaura homomalla allene oxide synthase 8R-LOX-fusion protein		3.51	**3DY5**	[49]
Human platelet-type 12-LOX	Incomplete structure	2.6	3D3L	Tresaugues et al. (to be published)

sion proteins, the LOX-domains are linked to the C-terminus of the other enzyme subunit. Thus, the C-terminal amino acid, which constitutes one of the five immediate iron ligands, remains free. This is of functional relevance since previous mutagenesis studies have indicated that C-terminal truncation of LOXs abolishes the enzymatic activity.

The small N-terminal LOX-domain is important for membrane binding and regulates the catalytic activity

The N-terminal domain (β-barrel domain) of all LOX-isoforms with available X-ray data has been seen to consist primarily of anti-parallel β-strands. Their overall structure resembles that of the C2-domain of pancreatic lipase, implicated in membrane binding [58]. For soybean LOX1, the β-barrel domain comprises the first 146 amino acid residues. In the case of rabbit 12/15-LOX and coral 8R-LOX, the β-barrel domains are formed from the N-terminal 110 amino acids or the first 114 residues, respectively. N- and C-terminal domains are covalently interconnected by a randomly-coiled oligopeptide. Although the β-barrel domains of the soybean LOX-isoforms are significantly larger than those of the animal enzymes, their overall structures are similar (Fig. 2). The N-terminal domain contacts the C-domain via an inter-domain contact plane, which amounts about 1600 Å2 for the rabbit 12/15-LOX [46]. This is significantly larger (2600 $Å^2$) for the soybean LOX1 suggesting that inter-domain binding forces may be stronger for this enzyme.

The high degree of conservation of the two-domain structure in LOXs suggests a functional role for the N-terminal β-barrel domain. Limited proteolysis of soybean LOX1 forms a truncated LOX lacking the N-terminal domain [59]. This "mini-LOX" is catalytically active and exhibits a decreased affinity for linoleic acid (*K*M of 24.2 μM for mini-LOX vs. 11.2 μM for native LOX). In contrast, V_{max} is augmented (363 s^{-1} for mini-LOX vs 55 s^{-1} for the native enzyme) and thus, the catalytic efficiency (k_{cat}/K_M) is improved by truncation. Recent studies indicated that the non-heme iron can be reversibly removed from the active site of mini-LOX, in contrast to the complete enzyme [60]. This indicates that N-terminal truncation alters the structure of the active site so that the iron falls off more easily [60]. Unfortunately, the mini-LOX has not been crystallized and a detailed description of the structural alterations induced by N-terminal truncation is not possible. Gene technical truncation of the N-terminal β-barrel domain of the rabbit 12/15-LOX [61] results in reduction of the catalytic efficiency (1.43 vs. 0.14 1/s μM). Interestingly, the truncation mutant undergoes more rapid suicidal inactivation during arachidonic acid oxygenation but the mechanisms involved are unknown. Taken together this data suggests that the N-terminal β-barrel domain is not essential for the catalytic activity, but may play a role in the regulation of turnover [61,62].

Due to its structural similarity to the β-barrel domain of human lipases [46,63], the N-terminal domains of plant and animal LOXs have been implicated in membrane binding [64,65]. Indeed, site-directed mutagenesis of surface-exposed tryptophans in the N-terminal domain inpairs membrane binding of the human 5-LOX and coral 8R-LOX [48,66]. For the rabbit 12/15-LOX, truncation of the β-barrel domain also reduces membrane binding but the isolated catalytic domain still binds to biomembranes, although to a lesser extend. Site-directed mutagenesis suggested that surface-exposed hydrophobic amino acids in both domains are involved in this process [61,67]. For soybean LOX1, proteolytic cleavage of the N-terminal β-barrel domain augments membrane binding [59].

Human 5-LOX requires Ca^{2+}-dependent membrane association for turnover [68,69]. Ca^{2+} also enhances membrane binding of rabbit 12/15-LOX but specific Ca^{2+}-binding amino acids do not appear to be involved [67,70]. Moreover, inspection of the β-barrel domain surface of the rabbit enzyme does not reveal the presence of specific calcium-binding motifs. In contrast, coral 8R-LOX contains specific calcium-binding sites in the β-barrel domain, formed by the side chains of Asp39 and Asp45 as well as Asp19, Asn44, and Glu47. These surface-exposed calcium-binding residues correspond to those proposed for the human 5-LOX and might initiate insertion of Trp41 and Trp77 into the phospholipid bilayer of membranes [48]. Since the calcium-binding residues and the two Trp are located on the same side as the putative entrance into the substrate-binding pocket, they may orient the catalytic domain to facilitate fatty acid acquisition from the membrane phase.

The C-terminal domain contains the substrate-binding pocket and the catalytic non-heme iron

The catalytic domain of all LOX-isoforms consists primarily of α-helices and harbors the catalytically active non-heme iron. For the soybean LOX1, helix 9 (comprising residues 473 through 518 with a length of 65 Å) is the central structural element [36]. Of

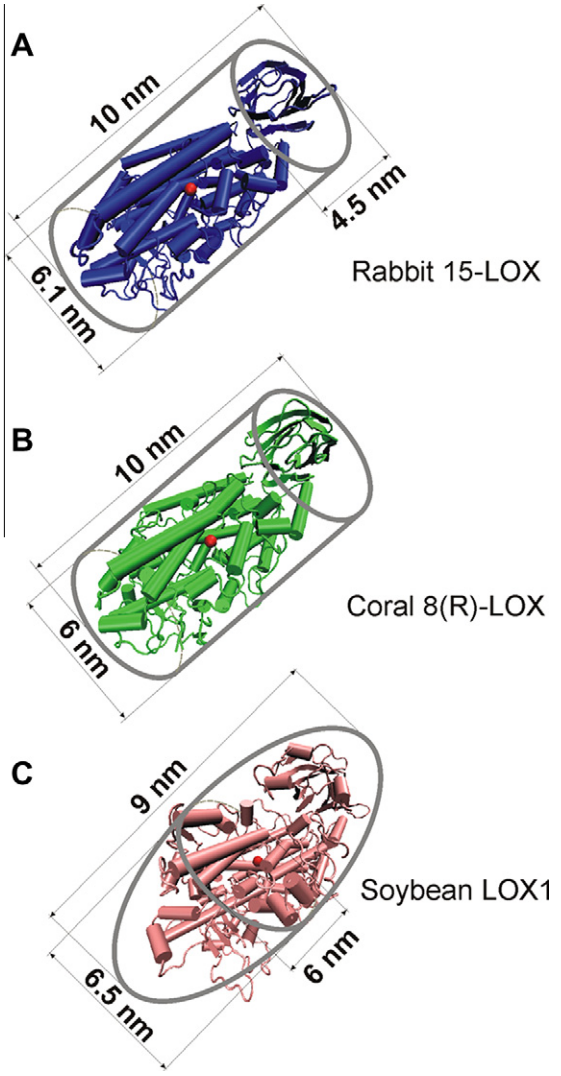

Fig. 2. Schematic structures of various LOX-isoforms. To design this scheme and others, we first overlaid three LOX structures to orient them the same way using the program VMD [159,160]. All isoforms show the characteristic two-domain structure and the N-terminal β-barrel domain is seen in the upper parts of the images. The catalytic non-heme iron is symbolized by the red dots. (A) The rabbit 12/15-LOX resembles an elliptic cylinder with a height of 10 nm. Its ground square has the dimension of about 6 nm and 4.5 nm. (B) The coral 8R-LOX has similar shape and dimensions as the rabbit 12/15-LOX. (C) The soybean LOX1 is an elliptic spheroid with similar dimensions as the other two LOX-isoforms.

the remaining helices, the longer ones are generally either parallel or anti-parallel to helix 9, so that the core of this domain represents a multihelix bundle. Two anti-parallel β-sheets are also present in the C-domain [36]. In the rabbit 12/15-LOX, the catalytic domain (residues 114-663) consists of 21 helices, interrupted by a small β-sheet sub-domain [46]. The catalytic domain of the coral enzyme (residues 115-694) involves 23 helices. In that enzyme, helix 2 is broken into two parts and is angled to a three-stranded anti-parallel β-sheet [34].

The catalytically active non-heme iron of all LOX-isoforms is octaedrically coordinated by five amino acid side chains and a hydroxide ligand. In case of soybean LOX1 and coral 8R-LOX, the protein iron ligands are three His, one Asn and the C-terminal Ile. In the crystal structure, the Asn is about 3 Å distant from the central iron and thus, its coordination forces are rather weak. However, detailed analysis of the X-ray coordinates [32] indicated the presence of an extensive hydrogen bonding network that connects the iron-ligating Asn via two second sphere residues (Gln495, Gln697) to another equatorial iron ligand (His499) [71]. In the rabbit 12/15-LOX, the iron is coordinated by four His and the C-terminal Ile [72]. One of these His (His545) aligns with the iron-liganding Asn of soybean LOX1, and is more distant from the central iron than the other ligands. As for the plant enzymes, its coordination forces are stabilized by a second sphere hydrogen bonding network, in which Glu357 (aligns with Gln495 of soybean LOX1) and Gln548 (aligns with Gln697 of soybean LOX1) participate [46].

The rabbit 12/15-LOX exhibits a high degree of motional flexibility but only limited data are currently available on the structural flexibility of other LOX-isoforms

In aqueous solutions the structure of macromolecules is much less rigid than in crystals. To compare the degree of motional flexibility of rabbit 12/15-LOX and soybean LOX1, small angle X-ray scattering (SAXS), dynamic fluorescence, and fluorescence resonance energy transfer measurements were carried out. The results suggest that rabbit 12/15-LOX is more susceptible to temperature-induced structural alterations and exhibits a higher degree of global conformational flexibility [73].

Interdomain-movement is a source of motional flexibility that is limited for the soybean LOX1

The X-ray coordinates for the soybean LOX1 suggest that the overall structures of the two domains are rather stable, and that there is little scope for major movement of secondary structural elements. The relatively large inter-domain contact plane (2.600 Å^2) [36] suggests intense non-covalent binding forces between the two domains which may arrest the N-terminal β-barrel domain at the catalytic subunit. Thus, the β-barrel domain may rock along the surface of the catalytic subunit but swinging away from it is unlikely [74]. This conclusion is consistent with SAXS data characterizing its solution structure. Thus, crystal and solution structures both indicate that in aqueous solutions, the N-terminal β-barrel domain remains arrested at the catalytic subunit [74].

The rabbit 12/15-LOX exhibits a higher degree of motional flexibility, with a smaller inter-domain contact plane than that of soybean LOX1 (1600 Å^2) [73]. Comparison of the SAXS data solution structure of the ligand-free rabbit 12/15-LOX (protein concentrations <1 mg/ml) with the crystallographic X-ray coordinates demonstrates an almost perfect alignment with the catalytic domain [75]. However, in the region of the N-terminal β-barrel domain the solution structure is stretched out. This indicates that the N-terminal β-barrel domain may temporarily swing away from the catalytic subunit. To test this hypothesis, similar X-ray scattering experiments were performed using a truncation mutant, in which the N-terminal β-barrel domain was deleted. For this mutant, the solution structure completely matched the crystallographic data.

The rabbit 12/15-LOX undergoes major conformational changes upon ligand binding at the active site

In the absence of ligands, the entrance to the putative substrate-binding pocket of rabbit 12/15-LOX is funnel-shaped and wide open. In fact, the catalytically active non-heme iron can be seen from the protein surface when looking into the substrate-binding pocket. On ligand binding, a condensed conformation is adopted, in which helix 2 (H2) is dislocated by approximately 12 Å (Fig. 3A) blocking the entrance into the substrate-binding pocket [47]. Displacement of H2 is paralleled by conformational alterations at the active site, whereby H18 retreats from the cavity enlarging the volume of the substrate-binding pocket. Thus, the triad constituents (see "The geometry of three crucial amino acids determine the positional specificity of 12/15-lipoxygenases (triad concept)") form the bottom of the substrate-binding pocket. This

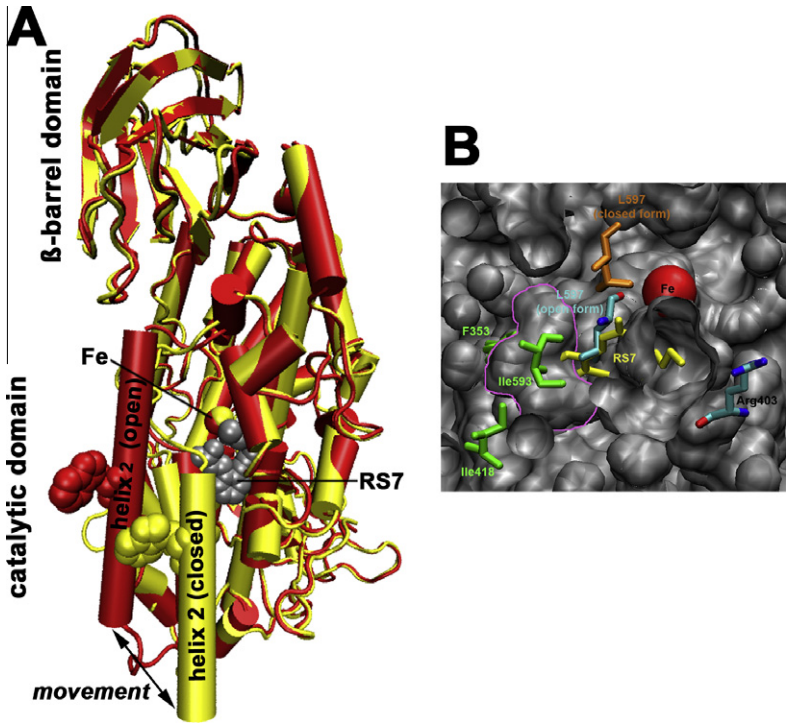

Fig. 3. Overlay of the two limit structures of the rabbit 12/15-LOX that are interchanged upon ligand binding. (A) The ligand-free open structure is indicated in red, the closed ligand-bound structure in yellow. The non-heme iron and the bound inhibitor (RS7) are also shown. It can be seen that helix H2 containing the surface-exposed W181, which has been implicated in membrane binding, is dislocated upon ligand binding by about 12 Å. (B) The surface for the open form structure was calculated [161] and the molecule sliced open to allow a view of internal cavities. The inhibitor RS7 from the overlaid closed structure is shown in yellow. The entrance to the substrate-binding pocket is still visible and Arg403, which interacts with the substrate's carboxylate, lies in close proximity. Leu597 separates the rather shallow entrance from the deeper part of the pocket contoured in pink and retracts about 6 Å upon ligand binding, thus giving access to this part. The triad residues F353, I418, and I593, determinants of the positional specificity by the volume of their side chains (see "The geometry of three crucial amino acids determine the positional specificity of 12/15-lipoxygenases (triad concept)"), are shown in green and the iron is given in red.

movement is also quite substantial, since the α-carbon atoms of Leu597 are separated by almost 6 Å [47] in both conformers (Fig. 3B). Comparing the positions of H2 in the two forms of the rabbit 12/15-LOX with the corresponding structural element of the coral 8R-LOX, it is apparent that the two conformers of the rabbit enzyme represent distinct extreme limit structures while 8R-LOX, although closer to the open form, represents an intermediate state [47].

This type of significant conformational alteration is unlikely in many plant LOXs, due to the tighter packing of the secondary structural elements. Indeed, superimposing the free and liganded forms of soybean LOX3 suggest that the amino acids between Leu331 and Gln341 juxtaposing helix 4 may be displaced slightly upon ligand binding, but that this movement does not exceed 3 Å. In contrast, H2 in the relaxed form of the rabbit enzyme is localized beneath helix 4 of soybean LOX3, while it overlays helix 2 in the condensed form [47].

The substrate-binding pocket is a hydrophobic cavity accessible from the protein surface

The hydrophobic nature of LOX fatty acid substrates suggests that predominantly hydrophobic residues line the substrate-binding pocket. Unfortunately, no direct structural information is available on LOX-substrate complexes. X-ray data characterizing the soybean LOX3–13S-HpODE complex [41] is unlikely to mirror a catalytically productive enzyme–substrate complex.

In addition to the inter-domain-crevice, the soybean LOX1 [35] contains two major cavities (cavity I and II), which intersect in the proximity of the non-heme iron. The side chains of Arg707 and Val354 (Fig. 4) separate cavity II into two subcavities (cavity IIa and IIb), sandwiched between two layers of helices (H9, H11 on one side, H2, H6, H18, H21 on the other). Cavity IIa that may function as substrate-binding pocket is intersected by a side-channel between Ile553 and Trp500, thought to target oxygen to the active site (Fig. 4). Site-directed mutagenesis studies suggest that Ile553 functions to limit oxygen availability [76]. However, more recent data implicate Ile553 in ensuring correct fatty acid alignment [31]. The entrance into the substrate-binding pocket (cavity IIa) is still a matter of discussion. Substrate fatty acids may penetrate the active site via movement of the side chains of Thr259 and Leu541 (Fig. 4) [36]. However, there does not appear to be any positively charged amino acid in this area that could form a salt-bridge with the fatty acid's carboxylate. The structures of various soybean LOX-isoforms (LOX1, LOX3, VLX-B, and VLX-D) demonstrate differences in shape and volume of cavity IIa. Polarity and bulkiness of the residues lining the pocket entrance are also distinct [39]. While cavity IIa in soybean LOX1 is a continuous channel, the corresponding structural element found in other soybean LOX-isoforms has barriers restricting substrate penetration [39].

The 3D-structure of the rabbit 12/15-LOX complexed with RS7 [46] was solved as enzyme–inhibitor complex. Unfortunately, important structural elements were not detected in the original electron density map. Recent reevaluation of the original X-ray coordinates [47] indicates a mixture of two different conformers, a ligand-free and a ligand-bound form. Comparison of their structures indicates that the enzyme undergoes substantial structural rearrangement upon ligand binding (see "The rabbit 12/15-LOX exhibits a high degree of motional flexibility but only limited data are currently available on the structural flexibility of other LOX-isoforms" and Fig. 3). In the ligand-free form (relaxed structure), the putative substrate-binding cavity is shallow, funnel-shaped

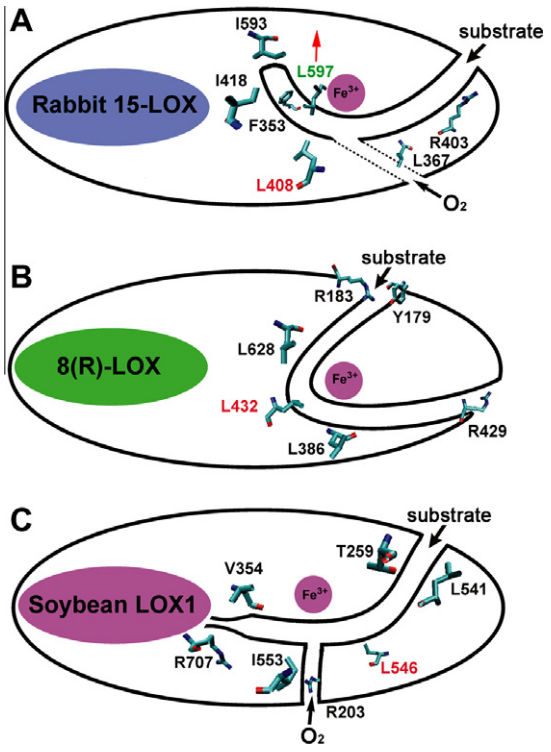

Fig. 4. Schematic comparison of the putative substrate-binding pocket in different LOX-isoforms and localization of important amino acids. The three LOX structures were overlaid using VMD [159,160]. Then the putative substrate-binding pocket was visualized and the position of functional amino acids were localized. (A) When fatty acids enter the substrate-binding pocket of the ligand-free (open) form of the enzyme, L597 appears to block deeper penetration so that the methyl end of the substrate may not contact the triad constituents (I418, F353, I593) (see "The geometry of three crucial amino acids determine the positional specificity of 12/15-lipoxygenases (triad concept)"). During ligand binding, the enzyme conformation is altered; L597 retracts and the substrate may slide in deeper into the substrate-binding pocket so that the methyl end of the substrate fatty acid gets in contact with the triad constituents which now prevent deeper penetration of the substrate (see also Fig. 3). R403 contacts the substrates' carboxylate and might initiate the conformational alterations [107]. The putative oxygen access channel intersects the substrate-binding pocket from behind and L367 is important for oxygen conductivity. L408, which is conserved in most LOXs (see also B, C red labels), was suggested to play an important role for proper substrate alignment. (B) For the coral 8R-LOX, substrate fatty acids may penetrate the active site between R183 and Y179, and R183 was suggested to interact with the substrates' carboxylate. L628, L432 and L386 line the substrate-binding channel to give it its characteristic U-shape. The exit of the U-shaped channel is closed by R429, but rearrangement of its side chain may open this back entrance to allow substrate penetration from the opposite end of the channel. (C) Cavity IIa was suggested to function as substrate-binding pocket of soybean LOX1, and fatty acids may penetrate this cavity with their methyl end ahead (tail-first orientation) between T259 and L541. Next, the fatty acid methyl end passes the conserved L546 and further slides in so that the bisallylic C13 of arachidonic acid is in close proximity to the iron. Cavity IIa is separated from cavity IIb by the side chain of R707 and V354. Oxygen was suggested to penetrate the active site via a side-channel lined by I553 and R203.

and reaches the protein surface around Arg403. In the ligand-bound form (condensed structure), the substrate-binding pocket is deeper, appearing as a bowed cavity concaved by the side chain of Leu408 (Fig. 4). The walls of the cavity are formed by 23 predominantly hydrophobic amino acids from six different helices (H2, H7, H9, H10, H16, and H18) and the loop connecting H9 and H10. The entrance into the substrate-binding pocket in the condensed conformation appears closed. Furthermore, Leu597 at the C-terminus of helix 18 appears to control the depth of the cavity (Figs. 3B and 4). In the ligand-free form, its side chain protrudes into the substrate-binding cavity thus limiting its depth and volume. This occupies the same space as the propanoic acid moiety of the inhibitor RS7 in the ligand-containing form. Upon ligand binding, helix 18 retreats by about 6 Å, resulting in the inner space of the binding pocket becoming available for substrate binding. Unfortunately, for this enzyme the functional importance of Leu408 and Leu597 for fatty acid oxygenation has not yet been explored experimentally.

The ligand-free coral 8R-LOX contains two well-resolved internal cavities forming a U-shaped channel that might allow access to the non-heme iron from opposite directions (Fig. 4). Leu628, aligns with the flexible Leu597 of the rabbit 12/15-LOX and constricts the channel separating two adjacent subcavities. Simultaneous movement of Tyr179, rotamer change of Leu386 and shift of Leu628 are required to open this constriction [47,48]. A positively charged Arg is located at both entrances into the U-shaped tunnel (Arg183 and Arg429), and this may interact with the fatty acid's carboxylate during substrate penetration of the active site. Arg429 forms a salt-bridge with Glu394 anchoring the arched helix (the roof of the channel) to the helical cluster of the catalytic domain. The other entry into the substrate-binding pocket near Arg183 is more likely to be functional, in line with the positional specificity of this isoform. While neither entrance is open in the crystal structure, the flexibility of the rabbit 12/15-LOX suggests that the absence of an obvious opening does not exclude fatty acid penetration. Site-directed mutagenesis studies of Arg183 and Arg429 would provide valuable information on the functionality of these residues, but these experiments have not been conducted yet.

Molecular dioxygen penetrates the active site via defined diffusion paths

Like other dioxygenases, LOXs catalyze a bimolecular reaction using atmospheric dioxygen as substrate. For a long time it was believed that oxygen can freely diffuse within proteins, so the question of how it may reach the catalytic center of LOXs was not addressed. However, recent data indicates an asymmetric oxygen distribution in proteins, and preformed oxygen diffusion channels were detected for various proteins [77–79]. For soybean LOX1, an oxygen access channel was suggested, and site-directed mutageneses as well as kinetic studies with selected enzyme mutants appear to confirm this concept. The putative substrate-binding pocket of soybean LOX1 (cavity IIa) is intersected by a side-channel (Fig. 4) bordered by Ile553. Structural modeling of an enzyme–substrate complex suggests that the site of intersection might be occupied by C13 of the linoleic acid radical formed during initial hydrogen abstraction. This putative oxygen access channel encounters the protein surface near Arg203 [36]. Thus, if this channel serves as path for diffusion, the oxygen molecule would directly be targeted from the solvent to its reaction site at the catalytic center. When Ile553 is mutated to a more bulky Phe, a 20-fold decrease in the catalytic efficiency ($k_{cat}/K_M[O_2]$) is observed [76,80]. This data is consistent with the working hypothesis that Ile553Phe exchange may limit oxygen diffusion. Ile553 of the soybean LOX aligns with Val439 of the coral 8*R*-LOX [34]. This amino acid is located at the C-terminal end of the arch that shelters the U-shaped substrate-binding channel. Although, the proximal part of the U-shaped cavity extending towards Arg429 was originally suggested as alternative fatty acid access channel into the active site, the possibility that it may function as oxygen access channel cannot be excluded. Unfortunately, there currently is no experimental data proving or disproving this hypothesis.

Inspection of the crystal structure of the rabbit 12/15-LOX shows that the putative soybean oxygen access channel is not conserved. To identify potential routes for oxygen diffusion, a 3D distribution map of the Gibbs free energy was calculated by placing a molecule of dioxygen from vacuum into any 1 $Å^3$ volume element of the enzyme protein, and then searching for low energy paths [81]. The global minimum of the energy distribution (oxygen high affinity area) is localized in close proximity to C15 of arachidonic

acid, in a model of the enzyme–substrate complex. Thus, the high affinity area coincides with the enzyme region where oxygen is utilized during catalysis. In fact, our simulations suggest that oxygen occupation probability within a 4 Å sphere around C15 of the arachidonic acid backbone is 7-fold higher than around C11. Thus, oxygen insertion at C15 appears to be favored over C11, consistent with the positional specificity of the enzyme. Three major channels interconnecting the protein surface with the oxygen high affinity area were identified for the substrate-free form by molecular dynamics simulations [81]. Path 1 starts at the bottom of the substrate-binding pocket, with its inner part corresponding to the oxygen channel postulated for soybean LOX1. This path is completely closed in the enzyme–substrate complex. The second path follows the substrate-binding pocket and is also blocked on substrate binding. The third channel (path 3) connects the opposite side of the protein molecule with the active site (Fig. 4). When arachidonic acid is added to the system, the global energy minimum is unaffected, and oxygen movement along path 3 does not change. Thus, only path 3 appears to be functional for both substrate-free and substrate–liganded forms. To provide experimental evidence for the functionality of this potential oxygen access channel, we attempted to reduce its oxygen conductivity by site-directed mutagenesis. For this, we mutated Leu367, which lines the putative oxygen access channel at a critical position (Fig. 4), to a more space filling Phe and demonstrated a 10-fold increased Michaelis constant for oxygen. The catalytic efficiency (k_{cat}/K_MO_2) for this mutant was 20-fold reduced; consistent with the hypothesis that path 3 may constitute a functional oxygen access channel [81].

The primary structure impacts the reaction specificity of fatty acid oxygenation and selected amino acids are of particular importance for different LOX-isoforms

The reaction specificity of LOX-isoforms with polyenoic fatty acids is the basis of the conventional LOX nomenclature. In mammals, arachidonic acid is used as model substrate whereas plant LOXs are usually categorized according to their specificity of linoleic acid oxygenation. Although the molecular basis for the reaction specificity of different LOX-isoforms has been explored in the past, there is no unifying concept applicable for all LOX-isoforms.

The way of substrate alignment at the active site is important for the reaction specificity

Polyenoic fatty acids are extremely flexible molecules with a large number of possible conformers. Thus, it is difficult to predict which conformation they adopt when bound at the active site. Experiments using synthetic fatty acid isomers suggest that for the soybean LOX1 [82] and the rabbit 12/15-LOX [83], the distance of the bisallylic methylene that serves as hydrogen donor from the methyl end of the substrate is of major importance. Based on the early soybean data a topological model for the alignment of fatty acids at the active site was developed [84], in which the methyl end of fatty acids penetrates into a hydrophobic substrate-binding pocket (tail-first model) so that the proS-hydrogen at C13 of arachidonic acid is localized in close proximity to the hydrogen acceptor (non-heme iron-bound hydroxyl). Three principle binding forces (hydrophobic-, π-electron-, ionic interactions) have been suggested that arrest free fatty acid substrates at the active site (Fig. 5). Modified substrates, such as 15S-HETE or its methyl ester appear to be inversely aligned so that the carboxylate enters the substrate-binding pocket. This "head-first" substrate orientation has heavily been debated in the past since it requires burying a positive charge in the hydrophobic environment of the substrate-binding pocket [85,86]. On the other hand, the X-ray data obtained for the soybean LOX3–13S-HpODE-complex [41] indicated the principle possibility of a "head-first" ligand binding when the carboxylate is liganded by a positively charged amino acid (Arg726 in case of soybean LOX3). In many plant LOXs this Arg is conserved, but in mammalian enzymes uncharged amino acids are located at this position. Additional evidence for the functional relevance of this Arg came from mutagenesis studies on the cucumber 13S-LOX [87]. For the wild-type enzyme, a tail-first substrate alignment was postulated, consistent with the stereochemistry of linoleic acid oxygenation. Here, the bulky side chain of His608 appears to shield the positively charged Arg758 so that no counterpart for interacting with the substrate's carboxylate is available. However, when His608 was mutated to a less bulky Val, Arg758 is deshielded and interacts with the fatty acid carboxylate to favor a "head-first" substrate alignment. Consequently, the mutant enzyme catalyzes predominantly linoleic acid 9S-oxygenation [87].

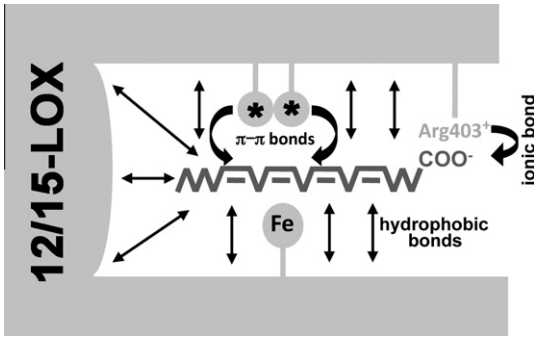

Fig. 5. Fatty acid alignment at the active site of 12/15-LOXs. Arachidonic acid slides into the substrate-binding pocket of 12/15-LOXs with its methyl end ahead and might be arrested at the active site by three principle binding forces: (i) ionic interactions of its carboxylate with Arg403. (ii) π–π-interactions of aromatic amino acid side chains (labeled with ∗) with the fatty acid double bonds, (iii) hydrophobic interactions of the hydrocarbon chain with hydrophobic residues lining the substrate-binding pocket. The catalytic non-heme iron is located between two bisallylic methylenes (C13 and C10) so that hydrogen abstraction is possible from either of them.

Summarizing the published data on fatty acid alignment at the active site of different LOX-isoforms, there appears to be the possibility of both, "tail-first" and "head-first" substrate binding. For a given isoform, equilibrium of both orientations is likely, although this steady state may be impacted by the nature of the substrate and by the reaction conditions [88–90]. Because of the possibility of unproductive substrate binding, the product pattern of fatty acid oxygenation does not necessarily mirror the binding equilibrium in quantitative terms. In other words, high product specificity does not exclude binding heterogeneity.

An alternative scenario of substrate alignment at the active site has recently been suggested for the coral 8R-LOX. Here, a U-shaped substrate-binding pocket was described, that reaches the protein surface with both ends [34] (Fig. 4). It was suggested that fatty acids may penetrate the active site in a "tail-first" way employing either of the two entrances. In both cases, the carboxylate remains outside the binding pocket. Unfortunately, for the time being there is no experimental data supporting the functionality of either entrance for this LOX-isoform.

Most S-LOXs have a conserved Ala at a critical position that is a Gly in R-LOXs

Hydrogen abstraction from the bisallylic methylene, and oxygen insertion into the rearranged fatty acid radical are two consecutive key reactions of LOX catalysis (Fig. 1). The two processes proceed from opposite directions of the plane determined by the double bond system of the fatty acid [5,91] (Fig. 6). This antarafacial stereochemistry suggests that hydrogen abstraction and oxygen insertion are coupled, but the molecular basis for this coupling has not been explored.

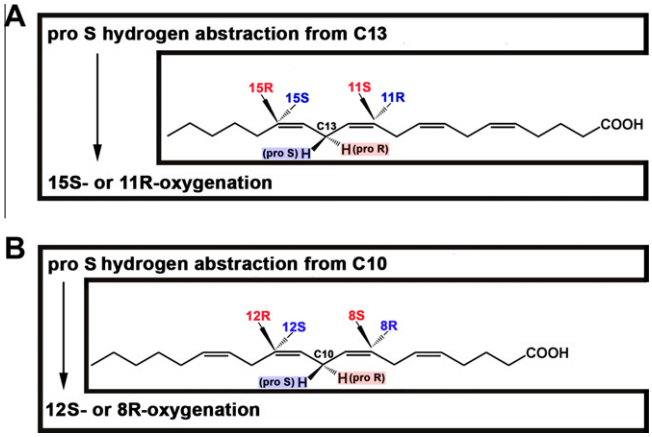

Fig. 6. Stereochemical aspects of LOX-catalyzed S- and R-lipoxygenation. (A) The pro S-hydrogen at C13 of arachidonic acid is localized in front of the plane of the pentadienyl double bonds. When LOXs catalyze abstraction of this proS-hydrogen, oxygen insertion proceeds from the opposite side of this plane (from behind). When oxygen insertion is preceded by a [+2] radical rearrangement, 15S-HpETE is formed. In contrast, when a [−2] rearrangement takes place 11R-HpETE results. In either case, oxygen was introduced from the same direction. The opposite designation is simply a result of the change in the priority order of the ligands at the asymmetric carbon atom, but does not reflect the direction of oxygen insertion. The major difference in the reaction mechanism of both enzymes is that the 15S-LOX catalyzes a [+2]-, the 11R-LOX a [-2]-radical rearrangement. (B) The same mechanistic considerations are true for 8R- and 12S-LOXs, with the exception that the proS-hydrogen is abstracted from C10. In contrast, mouse 8S-LOX and the 12R-LOXs remove the proR-hydrogen and oxygen is inserted from the opposite side of the double bond plane to give the 8S- and the 12R-products, respectively. These differences may be related to an inverse substrate orientation at the active site. In other words, in all LOXs oxygen comes from the same side, but an inversely oriented substrate results in opposite chirality (e.g. 8R/8S, 12R/12S).

Multiple amino acid alignments of various LOXs with known reaction specificity indicate that most S-LOXs contain an Ala at a critical position but in R-LOXs this amino acid is a Gly [3,92,93]. When Gly428 of the coral 8R-LOX is mutated to Ala, the predominant oxygenation product is 12S-HpETE. Similar observations were made for human [92] and mouse [94] 12R-LOX, but for the mouse enzyme the share of specific S-oxygenation products (8S-HpETE) only reaches about 40% [94]. When the inverse strategy was applied for the human 15S-LOX2 (Ala416Gly exchange), 11R-HpETE was identified as major reaction product (70%). Partial alterations in the enantioselectivity were also observed when corresponding mutations were carried out for the mouse 8S-LOX [92], soybean LOX1 [95], and Aribidopsis thaliana and tomato LOX [96]. When we performed corresponding mutagenesis studies on the rabbit 12/15-LOX, partial alterations in the reaction specificity were also observed. In fact, the major arachidonic acid oxygenation product of the Ala404Gly mutant remained 15S-H(p)ETE (75%) and 11R-H(p)ETE only contributed about 20% to the product profile. To explain the data, a mechanistic concept was developed [92] based on the assumption that oxygen penetration to the corresponding carbon atoms of the rearranged fatty acid radical may be sterically hindered. For instance, if a LOX abstracts the proS-hydrogen from C13 of arachidonic acid, the antarafacial character of the LOX-reaction prohibits oxygen insertion at the 15R- and 11S-positions (Fig. 6). Although the mechanistic basis for the antarafacial character is still unclear, it is possible that oxygen is just not available at these sites. Thus, oxygen may be inserted only at the 15S- or 11R-position, located at the same side of the fatty acid backbone. In 15S-LOXs, the Ala side chain has been suggested to block 11R oxygen insertion, favoring 15S-lipoxygenation. When Ala was mutated to a smaller Gly this hindrance is removed so that oxygen becomes available at the 11R-position. Unfortunately, this mechanism does not explain why Ala–Gly exchange reduces the share of 15S-oxygenation. This problem was overcome when the mechanism was refined on the basis of experimental data obtained for the coral 8R-LOX [34]. Here, the authors suggested that Leu432 blocks oxygen access either to the 12S- or the 8R-position (Fig. 6) depending on the spatial orientation of its side chain. In the wild-type enzyme, this side chain blocks the 12S-position. When Gly428 is mutated to Ala, the additional methyl group dislocates the side chain of Leu432, appearing to shield the 8R-position and making room for 12S-oxygenation. To test this concept, Leu432 in the coral 8R-LOX was mutated to a smaller Ala and a more bulky Phe [34], and the results appear to support the working hypothesis. However, the mutant enzyme species exhibit strongly reduced catalytic activities, making the data difficult to interpret. Moreover, Leu432 has also been implicated in correct fatty acid alignment at the active site and it is difficult to determine which of the two effects (fatty acid alignment, oxygen shielding) is more important. The principle problem with this hypothesis is that an Ala–Gly exchange does not induce a major gain of space. In fact, the van der Vaals volume of a methyl group (difference between Ala and Gly) amounts to about 20 $Å^3$ whereas a single molecule of dioxygen occupies a volume of about 50 $Å^3$. Thus, an Ala–Gly exchange does not even provide sufficient space for a single oxygen molecule. It is possible that the Ala might block the entrance into a preformed oxygen cavity, to be opened upon Ala–Gly exchange. Unfortunately, such preformed oxygen cavity has not been described for this enzyme and oxygen movement is difficult to monitor experimentally. However, since a high resolution structure is available for the coral 8R-LOX *in silico* calculations of intra-enzyme oxygen distribution [81] may be a suitable way to test the hypothesis indirectly. With this method it would be possible to quantify the probability of oxygen occupancy at different sites of the wild-type and the mutant enzyme. An alternative explanation for the effects induced by the Gly/Ala exchange may also be considered. The pentadienyl radical formed during initial hydrogen abstraction is usually considered as planar structure, in which the radical electron is delocalised over the entire double bond system. The preference of one position for oxygen insertion over another might be related to steric distortion of the planar moiety so that the electron density is forced on a certain carbon atom. Unfortunately, for the time being there is no direct experimental evidence for such distortion of the radical during the LOX-reaction.

For soybean LOX1, which converts linoleic acid almost exclusively to 13S-H(p)ODE, the Ala542Gly exchange induces formation of approximately 40% 9R-H(p)ODE. Wild-type enzyme and the Ala542Gly mutant abstract the same hydrogen and the fatty acid is bound with the same orientation [95]. Since oxygen also comes from the same direction the difference in product composition is simply a consequence of the inverse direction of radical rearrangement ([+2] for wild-type vs. [−2] for Ala542Gly mutant) (Fig. 6) and the resulting alterations in the priority orders of the ligands at the asymmetric carbon atom.

The geometry of three crucial amino acids determine the positional specificity of 12/15-lipoxygenases (triad concept)

For 12/15-LOXs, the triad concept provides a simple explanation of their reaction specificity. This hypothesis was first developed for the rabbit 12/15-LOX [97] and suggests that polyenoic fatty acids enter the substrate-binding pocket in the tail-first way (Fig. 5) with the carboxylate remaining outside to interact with Arg403. The bottom of the substrate-binding pocket (liganded form) is lined by the triad of Phe353, Ile418 and I593 and alterations in their side chain geometry modifies the volume of the pocket and thus fatty acid orientation at the active site. If the triad positions are occupied by small residues, fatty acid substrates are capable of penetrating deeper into the substrate-binding pocket so that hydrogen abstraction from C10 (12-lipoxygenation) is favored (Fig. 6 lower panel).

In contrast, if more space filling residues are located at these positions, hydrogen is mainly abstracted from C13 (15-lipoxygenation) (Fig. 6 upper panel). Site-directed mutagenesis studies on the following 12/15-LOXs support this concept: human 12/15-LOX [98,99], rabbit 12/15-LOX [97,100], rhesus monkey 12/15-LOX [101], orangutan 12/15-LOX [101], mouse 12/15-LOX [102], rat 12/15-LOX [103], and pig 12/15-LOX [104]. The relative importance of the triad constituents varies for different isoenzymes. For human and orangutan 12/15-LOXs, Phe353 and Ile418 (numbering according to the rabbit enzyme) play a major role since single mutations of these amino acids to less-space filling residues convert the enzyme to an almost completely 12-lipoxygenating enzyme. Consequently, these residues are considered first-order determinants. For the mouse 12/15-LOX, single mutations of the triad constituents induce only partial alterations of the positional specificity, but combined mutations are more effective. Similar observations were made for the human platelet 12-LOX, although even multiple mutations induce only minor alterations in specificity (14%) [101]. Studies on human 5-LOX indicated that simultaneous mutations of the triad constituents increase the share of 15S-oxygenation. In fact, for the quadruple mutant F359W + A424I + N425M + A603I 15S-H(p)ETE was identified as the dominant oxygenation product [105]. Although the mechanistic basis for these alterations is not known, the data indicate a 5-LOX can be converted to a 15-lipoxygenating enzyme by decreasing the volume of the substrate-binding pocket [105]. Mutagenesis data on the triad constituents of mouse 12R-LOX [94] and human 15-LOX2 [101] do not support the triad concept indicating that it may not be applicable for epidermis-type LOX-isoforms. Thus, this does not constitute a comprehensive model explaining the reaction specificity of all animal LOX-isoforms.

In silico models of the soybean LOX1–linoleate complex [95] suggested that the methyl end of the fatty acid deeply penetrates into the substrate-binding pocket to contact Phe557. This residue aligns with a second order triad constituent (Met419) of the rabbit enzyme and seems to be conserved as a bulky residue among plant 13-LOXs, whereas it is a smaller Val in plant 9-LOXs. Mutagenesis studies at this position with the cucumber 13S-LOX confirmed its importance for positional specificity [87] as described above. Furthermore, when Val542 of the cucumber lipid body LOX, which aligns with Phe353 of the rabbit enzyme, is mutated, the positional specificity is altered [106]. Taken together, this data suggests that the triad constituents may also play a role in substrate positioning in plant LOXs.

An improved model for the 12/15-LOX–arachidonic acid complex has recently been published [107] based on quantum-mechanical electronic structure calculations and molecular dynamics simulations. This supports the "boot-shaped" conformation of the substrate-binding cavity and confirms relocation of Leu597 upon substrate binding. It also suggests that sufficient space is available at the active site to allow conformational variability of arachidonic acid, in particular for alternative positioning of the double bond system. According to this, arachidonic acid is aligned at the active site with the C10 proS-hydrogen localized closer to the enzyme's proton acceptor (iron-bound hydroxyl) than the C13 proS-hydrogen. Nevertheless, during arachidonic acid oxygenation, abstraction of the C13 proS-hydrogen is strongly favored. The authors suggest that despite the spatial proximity, abstraction of the C10 proS-hydrogen is energetically hindered, and therefore C13-hydrogen removal is preferred.

The reaction specificity of human 15-LOX2 and its murine ortholog (8S-LOX) cannot be explained with the triad concept but two additional amino acid residues are of importance

Despite the fact that human 15-LOX2 and murine 8S-LOX have different positional specificities, they are ortholog enzymes with a high degree of sequence identity (78%). Two amino acid residues, Asp602 and Val603 in human 15-LOX2 (Tyr603 and His604 in murine 8S-LOX) have been identified as major sequence determinants for the positional specificity of these enzymes [108]. In contrast, mutation of the triad residues has little impact on the reaction specificity of epidermis-type LOX-isoforms [101]. The mechanistic basis for the different positional specificities of human 15-LOX2 and mouse 8S-LOX can be explained by opposite substrate orientation at the active site [89,108]. Human 15-LOX2 binds arachidonic acid in a "tail-first" way with hydrogen abstraction taking place at C13, followed by [+2] radical rearrangement, and oxygen insertion at C15 (Fig. 6). In contrast, murine 8S-LOX binds arachidonic acid in the "head-first" orientation involving C10 hydrogen abstraction, [−2] radical rearrangement, and oxygen insertion at C8. His604 is critical for inverse substrate orientation and is suggested to interact with the fatty acid's carboxylate [89,108].

There is no unifying mechanistic concept explaining the reaction specificity of all LOX-isoforms

The reaction specificity of a LOX is the consequence of the stereochemistry of the four elementary reactions (hydrogen abstraction, radical rearrangement, oxygen insertion, radical reduction). Because of the antarafacial character, hydrogen abstraction and oxygen insertion are mechanistically coupled but the structural basis for this coupling is unknown. However, it is unclear why certain LOXs catalyze a [+2] and others a [−2] radical rearrangement (Fig. 6). The carbon centered radical intermediate formed via hydrogen abstraction is usually depicted as a pentadienyl radical, in which the electron density is equally distributed over the entire pentadienyl moiety. However, if the electron density is focused at either of the carbon atoms, the oxygen acceptor site would be predetermined. There are several ways to achieve such predetermination:

(a) Electron drawing amino acids might localize the electron density of the fatty acid radical to focus it to a certain carbon atom of the pentadienyl system (*delocalizing hypothesis*).
(b) The planar pentadienyl radical is distorted, which may favor the formation of an en-allyl radical, in which the electron density is focused at a certain carbon atom (*distortion hypothesis*).
(c) Although the electron density may be equally distributed over the entire pentadienyl system, oxygen is selectively targeted to a certain carbon atom so that only a particular peroxy radical is formed (*oxygen targeting hypothesis*).
(d) If radical oxygenation is a reversible process and proceeds randomly, peroxy radical reduction might be stereoselective (*reduction hypothesis*).

Which of these mechanisms dominates for LOX-isoforms remains unclear, and it is possible that a combination of several causes is responsible for the high degree of reaction specificity of LOXs. Our molecular dynamics simulations of oxygen diffusion inside the rabbit 12/15-LOX suggest that the probability of oxygen occupancy at C15 of arachidonic acid is approximately 7-times higher than at C11. This is consistent with the positional specificity of the enzyme, but if guided oxygen diffusion is to be the only mechanism of stereocontrol, about 15% of 11-H(p)ETE should be detected as an arachidonic acid oxygenation product of the wild-type enzyme. This is clearly not the case for native rabbit 12/15-LOX. Moreover, our oxygen distribution maps usually show gradual alterations in the probability of oxygen occupancy within small (4–6 Å) radius spheres. In contrast, to explain the usually high positional specificity of most LOX-isoforms, a steep decline in the probability of oxygen occupancy within a small radius sphere should occur. In other words, the targeting hypothesis may con-

tribute to the positional specificity, but may not be the exclusive mechanism responsible for this enzyme property.

The reaction specificity of certain LOX-isoforms depends on the experimental conditions

It has been suggested that changes in reaction conditions may alter LOX specificity. In fact, pH alterations of the reaction buffer modify the positional specificity of plant LOXs [88,109]. Similar observations have recently been made for a LOX isolated from *Mormordica charantia* [110], but the structural basis for these changes remains unclear. Although pH alterations frequently occur in vivo, little is known of the impact on LOX specificity in animals. We recently investigated the pH-dependence of selected vertebrate LOXs, and observed a remarkable stability of the product pattern in the near physiological range [89]. However, subtle structural alterations induced by targeted mutagenesis and alterations in the substrate concentrations both induce a pronounced pH-dependence of the reaction specificity of some isoforms. For instance, for the V603H mutant of human 15-LOX2 8S-lipoxygenation is dominant (65%) at acidic pH, whereas 15S-H(p)ETE is the major oxygenation product at pH 8. Similarly, the product pattern of the wild-type mouse 8S-LOX is hardly altered in the near physiological pH range, but H604F exchange induces strong pH-dependent alterations in the positional specificity. Taken together, this data suggests that the specificity of LOXs depends on the reaction conditions, but the biological relevance of this remains unclear.

Allosteric regulation of LOX activity

LOXs are monomeric enzymes, and thus, allosteric regulation of their catalytic activity has never been explored in detail. For the human 5-LOX, allosteric regulation has been suggested with specific binding sites for ATP and Ca^{2+} [111]. However, it still remains unclear why ATP binding increases the catalytic activity of this enzyme. Kinetic studies on oxygenation of synthetic fatty acid sulfates by the human 12/15-LOX suggested allosteric regulatory mechanisms for this enzyme [112], and stopped-flow kinetics demonstrated that the regulators might not bind at the active site. The products of linoleic and arachidonic acid lipoxygenation altered the catalytic efficiency (k_{cat}/K_M) of human 15-LOX1 and 15-LOX2 [113,114]: The binding of 12-H(p)ETE or 13-H(p)ODE increased both the catalytic efficiency of arachidonic acid oxygenation related to linoleic acid oxygenation [increase in $(k_{cat}/K_M)^{AA}/(k_{cat}/K_M)^{LA}$ ratio] and the oxygen affinity of human 12/15-LOX1 for arachidonic acid oxygenation, while decreasing oxygen affinity for linoleic acid oxygenation [113]. Thus, in a cellular system where both fatty acids are simultaneously available, the binding of allosteric effectors might alter the substrate specificity (preference for arachidonic acid oxygenation). Interestingly, the catalytic activity of the soybean LOX1 was not affected by 15-HETE nor 13-HODE [115]. However, inhibitors of fatty acid oxygenation like oleyl- and palmitoleyl sulfate not only lowered the catalytic activity of the enzyme, but also altered the substrate specificity by increasing the arachidonic acid/linoleic acid ratio. This data suggests that both enzymes may undergo allosteric regulation but the molecular mechanism of this has not been clarified. It also remains unclear where the allosteric regulator might actually bind at the enzyme and what structural alterations ligand binding might induce.

The human platelet 12-LOX might occur as active dimer and exhibits a strong tendency for non-covalent oligomerization

SAXS data on both rabbit 12/15-LOX [75] and soybean LOX1 [74] suggest that the two enzymes occur as hydrated monomers in aqueous solutions at low protein concentrations (<1 mg/ml). This data is supported by native gel electrophoresis, gel filtration chromatography and mass spectrometry of the rabbit enzyme (Ivanov et al. unpublished data). With all these methods, we did not find convincing evidence for dimerization. It should, however, been stressed that at higher protein concentrations, which are far beyond physiologically relevant levels, the rabbit enzyme shows a tendency for irreversible protein aggregation. The molecular basis for this process remains unclear.

On the other hand, SAXS data on the human platelet 12-LOX suggested that this enzyme might occur as a dimer in aqueous solution. It also exhibits a tendency to aggregate into larger oligomers [116]. More detailed mechanistic studies suggest that oligomerization may be driven by the formation of intermolecular disulfide bridges, which are broken under reducing conditions. In contrast, enzyme dimers appear to be stable under reducing conditions excluding the importance of disulfide bridges [116]. Mass spectral analysis of the enzyme in aqueous solution indicated a protein with an apparent molecular mass of 77 kDa, characteristic of enzyme monomers. The apparent contradiction between the SAXS data and the mass spectral analysis might be explained by the fact that the non-covalently linked dimers are thermodynamically unstable during mass spectral analysis.

Evolutionary aspects of LOXs

Lipoxygenase sequences are present in eucaryotes and bacteria but not in archea

LOXs are widely distributed in plants [8,117], mammals [1,101] and selected marine organisms [118,119]. More recently, LOX-isoforms have been detected in various prokaryotes [120–122]. To obtain more detailed information on the LOX distribution, we searched various databases (GenBank, Refseq, Uniprot, Ensembl) for LOX-specific sequences. Unfortunately, the LOX family is structurally quite heterogeneous, since cDNA or protein alignments of known LOX-isoforms indicate that there is no joint characteristic sequence that is shared by all. For our search we employed the sequences representing the region surrounding the direct iron ligands and show the highest degree of conservation. The positive results were sorted according to kingdom and phylum, and examples for different biological orders are given in Fig. 7. LOX sequences can be found in two of the three kingdoms of life (eukaryotes, prokaryotes). In the third, the archaea, no LOX was detected which is not surprising considering their extreme habitats. In fact, for many archaea, the LOX substrate molecular dioxygen is toxic. It should be stressed that detection of a LOX-related sequence does not necessarily mean that an active enzyme is actually expressed. Moreover, classification of the sequences into the different subfamilies (12/15-LOX, platelet-type 12-LOX, 5-LOX, epidermal type LOXs) is not possible on the sole basis of sequence information.

During evolution, LOXs have arisen in several prokaryotes (cyanobacteria and proteobacteria), in unicellular protista (red and green algae, the amoeba *Dictyostelium discoideum*), fungi, plants (mosses as well as flowering plants) and animals (Fig. 7). In animals, LOX sequences occur in many species ranging from the very basic placozoa *Trichoplax adhaerens* up to primates and include, among others, coral, tick, acorn worm, fish, frog, chicken, bat, hedgehog, mouse, dolphin, elephant, monkey, and human.

Many of the LOX-containing species serve as model organisms representing certain developmental stages of eukaryotes. *Volvox carteri* is one of the most basic multicellular organisms that still exist, and *T. adhaerens* is one of the most basic eumetazoa, being closely related to Cnidaria [123]. Other model organisms containing

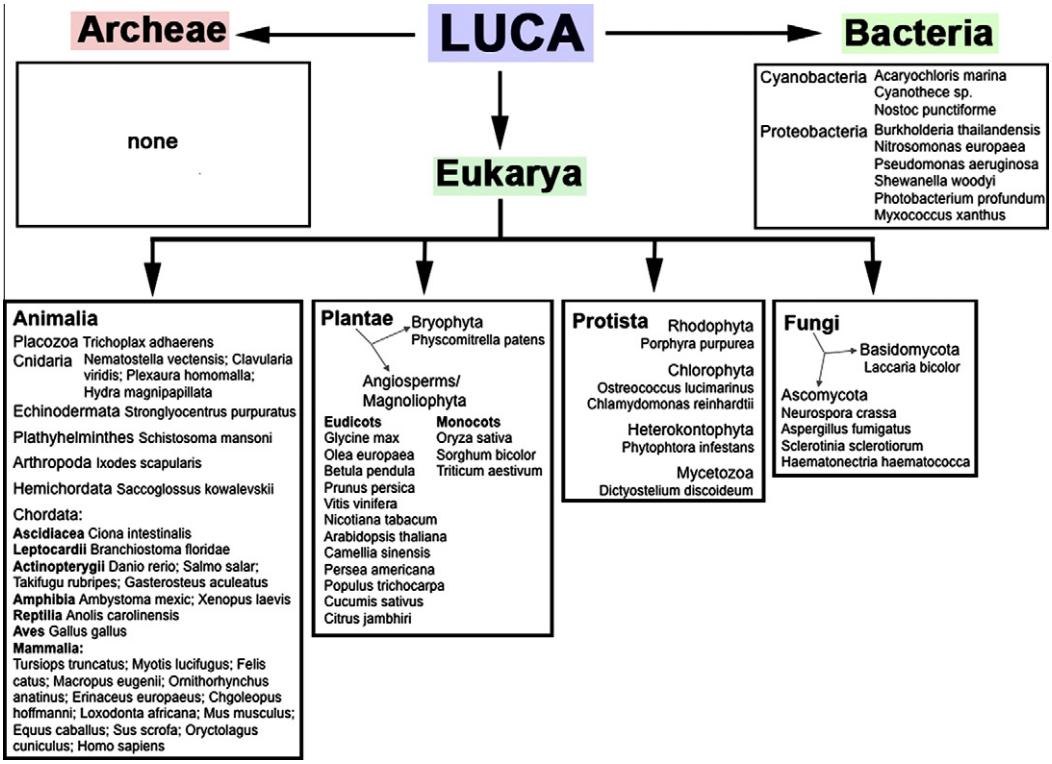

Fig. 7. Distribution of LOX sequences in various kingdoms of life. LOX sequences have been detected in prokaryotic (bacteria) and eukaryotic (protista, fungi, plantae and animalia), but not in archaea. Only examples for different orders are given. LUCA, last universal common ancestor.

LOXs are the amoeba *D. discoideum* (model organism for cell differentiation, chemotaxis and apoptosis), the vase tunicate *Ciona intestinalis* (is considered the closest invertebrate relative to humans, shares about 80% of human genes), the lancelet *Branchiostoma floridae* (appears to be most closely related to the archetypal vertebrate), and the pufferfish *Tetraodon nigroviridis* (smallest known vertebrate genome, 340 million bp). The zebrafish *Danio rerio*, frequently used in vertebrate developmental and gene function studies, contains several LOX sequences, with some having been classified to 12- and 5-LOX on the basis of amino acid sequence conservation. In the genome of other model organisms like *Saccharomyces cerevisiae, Caenorhabditis elegans*, and *Drosophila melanogaster,* no LOX-related sequence was found.

Is there a common LOX ancestor?

With a few exceptions, e.g. the cyanobacterium *A. marina*, in which five different LOX sequences have been detected, unicellular organisms mostly contain just one or two LOXs. In contrast, mice have seven functional LOX genes and expression of a number of splice variants augments the isoform-multiplicity. *Arabidopsis thaliana*, a model organism of higher plants, contains 6 LOX genes [124] and some plants even contain more than 15 different LOX sequences. It remains unclear why such multiplicity has evolved in higher organisms. Sequence comparison of LOX-isoforms in a given species suggested that at least some of the different isoforms evolved by gene duplications [125,126]. However, it remains an open question whether there is an ancient LOX precursor and which of the current isoforms is most closely related to this hypothetical enzyme species.

When the first LOX sequences in bacteria were described, the possibility of a horizontal gene transfer was discussed [120]. Although many of the unicellular organisms are pathogens or symbionts and thus get in close contact with plants or animals, the number and the heterogeneity of LOX-isoforms in lower organisms strongly suggest that a horizontal gene transfer may not be the only explanation for prokaryotic LOXs. It is more plausible that pro- and eukaryotic LOXs evolved from a common ancient precursor. Cyanobacteria are amongst the oldest forms of life on earth. They are believed to be responsible for converting the ancient atmosphere to an oxidizing environment due to their ability to conduct oxygenic photosynthesis and release molecular oxygen. LOXs occur in different orders of cyanobacteria [55,56,122,127–130], indicating an early development of these enzymes during evolution. Thus, it may well be that the first LOXs were expressed in cyanobacteria. According to the endosymbiotic theory, cyanobacteria are the origin of chloroplasts [131,132] and in many cases a transfer of plastid genes into the nuclear genome has occurred [133–137]. In this way, LOXs could have evolved in plants and indeed, some current plant LOX-isoforms have plastidal localization sequences. Recently, LOXs were found in other plastids, including the chromoplasts of ripe tomatoes [138]. However, no LOX sequences have been detected in Rickettsia and Alpha proteobacteria that have been related to the endosymbiotic theory of mitochondria [139].

Another aspect of more recent LOX evolution is the hypothesis that only 12/15-LOXs from hominidae (human, chimpanzee, orangutan, and gorilla) are 15-lipoxygenating enzyme species. Although the positional specificities of chimpanzee and gorilla LOX have not been tested experimentally, sequence comparison of the triad constituents suggest arachidonic acid 15-lipoxygenation. In contrast, other mammals (e.g. *Macaca mulatta*, pig, mouse, rat) express 12-lipoxygenating 12/15-LOX-isoforms [101,140–143]. The only exception from this rule is the rabbit where genes encoding a 12- and a 15-lipoxygenating 12/15-LOX have been described [144]. Whether this switch to arachidonic acid 15-lipoxygenation during mammalian LOX evolution is of functional importance remains to be explored.

The biological role of LOX-isoforms in lower organisms remains unclear

The biological function of mammalian LOXs has been explored by targeted knockout of the corresponding genes. Mice in which the 12/15-LOX gene [145], the 5-LOX gene [146] or the platelet-type 12-LOX gene [147] is disrupted, are viable and develop normally. This also applies for a 12/15-LOX + 5-LOX double knockout [148]. In plants, LOXs have been implicated in numerous functions (see Ref. [149] and [150] for a review) which include the production of phytohormons [151], seed germination [152], leaf senescence [153,154], and flavor development [155,156]. However, it remains unclear why certain plants express such a large variety of LOX-isoforms.

In lower organisms the biological role of LOXs has not been explored in detail. In the coral *P. homomalla,* the enzyme has been implicated in the generation of prostaglandins [157] which amount from 2% to 3% of the organisms dry weight. Unfortunately, the biological role of this prostaglandin derivative for coral physiology has not yet been clarified. When cyanobacteria are wounded by sonication, formation of endogenous LOX products is strongly increased [128]. In other lower organisms, LOX-isoforms have been implicated in defense mechanisms, stress responses or cell differentiation and maturation but in general the molecular mechanisms have not been well elucidated.

Future development and perspective

In 1993 the crystal structure of the soybean LOX1 was solved, and in the following years X-ray coordinates for additional isoforms were published (Table 1). On the basis of this data, it is now possible to model the principle 3D-structure of other isoforms and a model for the potato 5-LOX has been suggested [158]. However, it is dangerous and can be misleading to conclude structural details and functional consequences of structural peculiarities simply on the basis of sequence similarity and in the absence of functional data. Although such functional data are sometimes difficult to interpret, they are needed to confirm or disprove working hypotheses.

A hallmark in recent LOX structural biology was the reinterpretation of the original X-ray coordinates of the rabbit 12/15-LOX–inhibitor complex [47]. This report demonstrates that LOXs are dynamic structures that undergo conformational alterations upon ligand binding. These changes are quite impressive and impact both the protein surface (12 Å movement of H2) and the structure of the putative substrate-binding pocket (6 Å movement of Leu597). This data strongly suggests functional consequences of these structural alterations. Moreover, when we inspected the internal cavity system of the relaxed (ligand-free) and the condensed (ligand-bound) enzyme structure in more detail, we found marked differences. In the relaxed structure, the triad constituents are not part of the substrate-binding pocket, which is strongly narrowed by the side chain of Leu597. However, in the condensed structure, Leu597 is dislocated to further open the pocket so that the substrate fatty acid can contact the triad constituents, in agreement with the mutagenesis data [97,100]. Although the dynamic character of the rabbit enzyme is consistent with X-ray scattering and dynamic fluorescence data, it remains unclear whether other LOX-isoforms exhibit a similar degree of motional flexibility. Dynamic measurements of structural alterations in other LOX-isoforms are required to address this open question.

Another open point in the structural biology of LOXs is the biological importance of the N-terminal β-barrel domain. Mutagenesis and limited proteolysis have implicated this domain in membrane binding and activity regulation. However, the molecular basis for this function remains unclear. Although the catalytic domain of LOXs appears to be a structurally stable unit, it cannot be excluded that N-terminal truncation may lead to structural alterations in the catalytic domain responsible for the alterations in the catalytic activity. Unfortunately, nothing is known on the structure of truncated LOX-isoforms. To clarify this point it would be helpful to have direct structural data on the mini-LOX, which is produced from soybean LOX1 by limited proteolysis.

The biological relevance of LOX-isoforms in higher plants and animals has been a matter of discussion for many years and knockout studies have advanced the field in several ways. The recent discovery of LOX-isoforms in lower organisms and even in prokaryotes might speed up this development. There are, however, two major problems: (i) At the moment little is known on the biological function of such LOX-isoforms. In fact, except from rare cases it remains unclear of whether or not the detected LOX sequences are actually expressed as functional proteins. Moreover, many of them have not even been characterized with respect to their enzymatic properties. (ii) If in the future, experimental data on the biological relevance of such LOX-isoforms becomes available, it remains unclear what we can learn from such findings for the biology of LOXs in higher plants and animals. However, lower organisms are easier to handle and loss and gain-of-function strategies are more straightforward then corresponding experiments in higher species. Thus, irrespective of the uncertainties discussed above, more knowledge on the biology of LOXs in lower organisms is expected to boost LOX research in general.

References

[1] A.R. Brash, J. Biol. Chem. 274 (1999) 23679–23682.
[2] H. Kuhn, J. Saam, S. Eibach, H.G. Holzhutter, I. Ivanov, M. Walther, Biochem. Biophys. Res. Commun. 338 (2005) 93–101.
[3] C. Schneider, D.A. Pratt, N.A. Porter, A.R. Brash, Chem. Biol. 14 (2007) 473–488.
[4] M.H. Glickman, J.P. Klinman, Biochemistry 34 (1995) 14077–14092.
[5] K.W. Rickert, J.P. Klinman, Biochemistry 38 (1999) 12218–12228.
[6] N. Lehnert, E.I. Solomon, J. Biol. Inorg. Chem. 8 (2003) 294–305.
[7] E. Hatcher, A.V. Soudackov, S. Hammes-Schiffer, J. Am. Chem. Soc. 126 (2004) 5763–5775.
[8] A. Andreou, I. Feussner, Phytochemistry 70 (2009) 1504–1510.
[9] J.M. Upston, J. Neuzil, P.K. Witting, R. Alleva, R. Stocker, J. Biol. Chem. 272 (1997) 30067–30074.
[10] Y. Takahashi, W.C. Glasgow, H. Suzuki, Y. Taketani, S. Yamamoto, M. Anton, H. Kuhn, A.R. Brash, Eur. J. Biochem. 218 (1993) 165–171.
[11] T. Schewe, W. Halangk, C. Hiebsch, S.M. Rapoport, FEBS Lett. 60 (1975) 149–152.
[12] B. Samuelsson, P. Borgeat, S. Hammarstrom, R.C. Murphy, Adv. Prostaglandin Thromboxane Leukotriene Res. 6 (1980) 1–18.
[13] B.A. Jakschik, L.H. Lee, Nature 287 (1980) 51–52.
[14] S. Feltenmark, N. Gautam, A. Brunnstrom, W. Griffiths, L. Backman, C. Edenius, L. Lindbom, M. Bjorkholm, H.E. Claesson, Proc. Natl. Acad. Sci. USA 105 (2008) 680–685.
[15] C.N. Serhan, M. Hamberg, B. Samuelsson, Proc. Natl. Acad. Sci. USA 81 (1984) 5335–5339.
[16] P. Maderna, C. Godson, Br. J. Pharmacol. 158 (2009) 947–959.
[17] C.N. Serhan, K. Gotlinger, S. Hong, M. Arita, Prostaglandins Other Lipid Mediators 73 (2004) 155–172.
[18] A. Ariel, P.L. Li, W. Wang, W.X. Tang, G. Fredman, S. Hong, K.H. Gotlinger, C.N. Serhan, J. Biol. Chem. 280 (2005) 43079–43086.
[19] J.M. Schwab, N. Chiang, M. Arita, C.N. Serhan, Nature 447 (2007) 869–874.
[20] C.N. Serhan, R. Yang, K. Martinod, K. Kasuga, P.S. Pillai, T.F. Porter, S.F. Oh, M. Spite, J. Exp. Med. 206 (2009) 15–23.
[21] G. Furstenberger, N. Epp, K.M. Eckl, H.C. Hennies, C. Jorgensen, P. Hallenborg, K. Kristiansen, P. Krieg, Prostaglandins Other Lipid Mediators 82 (2007) 128–134.
[22] N. Epp, G. Furstenberger, K. Muller, J. Cell Biol. 177 (2007) 173–182.
[23] K.M. Eckl, J. Invest. Dermatol. 129 (2009) 1421–1428.
[24] S. Bhattacharya, G. Mathew, D.G. Jayne, S. Pelengaris, M. Khan, Tumour Biol. 30 (2009) 185–199.
[25] G.P. Pidgeon, J. Lysaght, S. Krishnamoorthy, J.V. Reynolds, K. O'Byrne, D. Nie, K.V. Honn, Cancer Metastasis Rev. 26 (2007) 503–524.
[26] J.J. Moreno, Biochem. Pharmacol. 77 (2009) 1–10.
[27] Y. Chawengsub, K.M. Gauthier, W.B. Campbell, Am. J. Physiol. Heart Circ. Physiol. 297 (2009) H495–H507.
[28] N. Mochizuki, Y.G. Kwon, Circ. Res. 102 (2008) 143–145.
[29] N.P. Duroudier, A.S. Tulah, I. Sayers, Allergy 64 (2009) 823–839.

[30] M. Hersberger, Clin. Chem. Lab. Med. (2008).
[31] M.P. Meyer, D.R. Tomchick, J.P. Klinman, Proc. Natl. Acad. Sci. USA 105 (2008) 1146–1151.
[32] D.R. Tomchick, P. Phan, M. Cymborowski, W. Minor, T.R. Holman, Biochemistry 40 (2001) 7509–7517.
[33] E.N. Segraves, M. Chruszcz, M.L. Neidig, V. Ruddat, J. Zhou, A.T. Wecksler, W. Minor, E.I. Solomon, T.R. Holman, Biochemistry 45 (2006) 10233–10242.
[34] D.B. Neau, N.C. Gilbert, S.G. Bartlett, W. Boeglin, A.R. Brash, M.E. Newcomer, Biochemistry 48 (2009) 7906–7915.
[35] J.C. Boyington, B.J. Gaffney, L.M. Amzel, Biochem. Soc. Trans. 21 (Pt 3) (1993) 744–748.
[36] W. Minor, J. Steczko, B. Stec, Z. Otwinowski, J.T. Bolin, R. Walter, B. Axelrod, Biochemistry 35 (1996) 10687–10701.
[37] E. Skrzypczak-Jankun, L.M. Amzel, B.A. Kroa, M.O. Funk Jr., Proteins 29 (1997) 15–31.
[38] E. Skrzypczak-Jankun, O.Y. Borbulevych, M.I. Zavodszky, M.R. Baranski, K. Padmanabhan, V. Petricek, J. Jankun, Acta Crystallogr. Sect. D Biol. Crystallogr. 62 (2006) 766–775.
[39] B. Youn, G.E. Sellhorn, R.J. Mirchel, B.J. Gaffney, H.D. Grimes, C. Kang, Proteins 65 (2006) 1008–1020.
[40] E. Skrzypczak-Jankun, K. Zhou, N.P. McCabe, S.H. Selman, J. Jankun, Int. J. Mol. Med. 12 (2003) 17–24.
[41] E. Skrzypczak-Jankun, R.A. Bross, R.T. Carroll, W.R. Dunham, M.O. Funk Jr., J. Am. Chem. Soc. 123 (2001) 10814–10820.
[42] O.Y. Borbulevych, J. Jankun, S.H. Selman, E. Skrzypczak-Jankun, Proteins 54 (2004) 13–19.
[43] E. Skrzypczak-Jankun, K. Zhou, J. Jankun, Int. J. Mol. Med. 12 (2003) 415–420.
[44] E. Skrzypczak-Jankun, O.Y. Borbulevych, J. Jankun, Acta Crystallogr. Sect. D Biol. Crystallogr. 60 (2004) 613–615.
[45] C. Pham, J. Jankun, E. Skrzypczak-Jankun, R.A. Flowers 2nd, M.O. Funk Jr., Biochemistry 37 (1998) 17952–17957.
[46] S.A. Gillmor, A. Villasenor, R. Fletterick, E. Sigal, M.F. Browner, Nat. Struct. Biol. 4 (1997) 1003–1009.
[47] J. Choi, J.K. Chon, S. Kim, W. Shin, Proteins 70 (2008) 1023–1032.
[48] M.L. Oldham, A.R. Brash, M.E. Newcomer, J. Biol. Chem. 280 (2005) 39545–39552.
[49] N.C. Gilbert, M. Niebuhr, H. Tsuruta, T. Bordelon, O. Ridderbusch, A. Dassey, A.R. Brash, S.G. Bartlett, M.E. Newcomer, Biochemistry 47 (2008) 10665–10676.
[50] R. Koljak, O. Boutaud, B.H. Shieh, N. Samel, A.R. Brash, Science 277 (1997) 1994–1996.
[51] O. Boutaud, A.R. Brash, J. Biol. Chem. 274 (1999) 33764–33770.
[52] B.D. Abraham, M. Sono, O. Boutaud, A. Shriner, J.H. Dawson, A.R. Brash, B.J. Gaffney, Biochemistry 40 (2001) 2251–2259.
[53] M.L. Oldham, A.R. Brash, M.E. Newcomer, Proc. Natl. Acad. Sci. USA 102 (2005) 297–302.
[54] H. Lohelaid, R. Jarving, K. Valmsen, K. Varvas, M. Kreen, I. Jarving, N. Samel, Biochim. Biophys. Acta 1780 (2008) 315–321.
[55] Y. Zheng, W.E. Boeglin, C. Schneider, A.R. Brash, J. Biol. Chem. 283 (2008) 5138–5147.
[56] C. Schneider, K. Niisuke, W.E. Boeglin, M. Voehler, D.F. Stec, N.A. Porter, A.R. Brash, Proc. Natl. Acad. Sci. USA 104 (2007) 18941–18945.
[57] B. Gao, W.E. Boeglin, Y. Zheng, C. Schneider, A.R. Brash, J. Biol. Chem. 284 (2009) 22087–22098.
[58] H. Chahinian, B. Sias, F. Carriere, Curr. Protein Pept. Sci. 1 (2000) 91–103.
[59] M. Maccarrone, M.L. Salucci, Biochemistry 40 (2001) 6819–6827.
[60] E. Dainese, C.B. Angelucci, A. Sabatucci, V. De Filippis, G. Mei, M. Maccarrone, FASEB J. 24 (2010) 1725–1736.
[61] M. Walther, M. Anton, M. Wiedmann, R. Fletterick, H. Kuhn, J. Biol. Chem. 277 (2002) 27360–27366.
[62] S. Romanov, R. Wiesner, G. Myagkova, H. Kuhn, I. Ivanov, Biochemistry 45 (2006) 3554–3562.
[63] F.K. Winkler, A. D'Arcy, W. Hunziker, Nature 343 (1990) 771–774.
[64] C. May, M. Hohne, P. Gnau, K. Schwennesen, H. Kindl, Eur. J. Biochem. 267 (2000) 1100–1109.
[65] S.A. Tatulian, J. Steczko, W. Minor, Biochemistry 37 (1998) 15481–15490.
[66] S. Kulkarni, S. Das, C.D. Funk, D. Murray, W. Cho, J. Biol. Chem. 277 (2002) 13167–13174.
[67] M. Walther, R. Wiesner, H. Kuhn, J. Biol. Chem. 279 (2004) 3717–3725.
[68] T. Hammarberg, P. Provost, B. Persson, O. Radmark, J. Biol. Chem. 275 (2000) 38787–38793.
[69] X.S. Chen, C.D. Funk, The. N-terminal, J. Biol. Chem. 276 (2001) 811–818.
[70] R. Brinckmann, K. Schnurr, D. Heydeck, T. Rosenbach, G. Kolde, H. Kuhn, Blood 91 (1998) 64–74.
[71] G. Schenk, M.L. Neidig, J. Zhou, T.R. Holman, E.I. Solomon, Biochemistry 42 (2003) 7294–7302.
[72] R.J. Kuban, R. Wiesner, J. Rathman, G. Veldink, H. Nolting, V.A. Sole, H. Kuhn, Biochem. J. 332 (Pt 1) (1998) 237–242.
[73] G. Mei, A. Di Venere, E. Nicolai, C.B. Angelucci, I. Ivanov, A. Sabatucci, E. Dainese, H. Kuhn, M. Maccarrone, Biochemistry 47 (2008) 9234–9242.
[74] E. Dainese, A. Sabatucci, J. Mol. Biol. 349 (2005) 143–152.
[75] M. Hammel, M. Walther, R. Prassl, H. Kuhn, J. Mol. Biol. 343 (2004) 917–929.
[76] M.J. Knapp, J.P. Klinman, Biochemistry 42 (2003) 11466–11475.
[77] K. Chu, J. Vojtchovsky, B.H. McMahon, R.M. Sweet, J. Berendzen, I. Schlichting, Nature 403 (2000) 921–923.
[78] A. Ostermann, R. Waschipky, F.G. Parak, G.U. Nienhaus, Nature 404 (2000) 205–208.
[79] E.E. Scott, Q.H. Gibson, Biochemistry 36 (1997) 11909–11917.
[80] M.J. Knapp, F.P. Seebeck, J.P. Klinman, J. Am. Chem. Soc. 123 (2001) 2931–2932.
[81] J. Saam, I. Ivanov, M. Walther, H.G. Holzhutter, H. Kuhn, Proc. Natl. Acad. Sci. USA 104 (2007) 13319–13324.
[82] M. Hamberg, B. Samuelsson, J. Biol. Chem. 242 (1967) 5329–5335.
[83] H. Kuhn, H. Sprecher, A.R. Brash, J. Biol. Chem. 265 (1990) 16300–16305.
[84] H. Kuhn, T. Schewe, S.M. Rapoport, Adv. Enzymol. Relat. Areas Mol. Biol. 58 (1986) 273–311.
[85] M. Browner, S.A. Gillmor, R. Fletterick, Nat. Struct. Biol. 5 (1998) 179.
[86] S.T. Prigge, B.J. Gaffney, L.M. Amzel, Nat. Struct. Biol. 5 (1998) 178–179.
[87] E. Hornung, M. Walther, H. Kuhn, I. Feussner, Proc. Natl. Acad. Sci. USA 96 (1999) 4192–4197.
[88] H.W. Gardner, Biochim. Biophys. Acta 1001 (1989) 274–281.
[89] M. Walther, J. Roffeis, C. Jansen, M. Anton, I. Ivanov, H. Kuhn, Biochim. Biophys. Acta (2009).
[90] M. Walther, I. Ivanov, G. Myagkova, H. Kuhn, Chem. Biol. 8 (2001) 779–790.
[91] R.L. Maas, A.R. Brash, Proc. Natl. Acad. Sci. USA 80 (1983) 2884–2888.
[92] G. Coffa, A.R. Brash, Proc. Natl. Acad. Sci. USA 101 (2004) 15579–15584.
[93] G. Coffa, C. Schneider, A.R. Brash, Biochem. Biophys. Res. Commun. 338 (2005) 87–92.
[94] S. Meruvu, M. Walther, I. Ivanov, S. Hammarstrom, G. Furstenberger, P. Krieg, P. Reddanna, H. Kuhn, J. Biol. Chem. 280 (2005) 36633–36641.
[95] G. Coffa, A.N. Imber, B.C. Maguire, G. Laxmikanthan, C. Schneider, B.J. Gaffney, A.R. Brash, J. Biol. Chem. 280 (2005) 38756–38766.
[96] W.E. Boeglin, A. Itoh, Y. Zheng, G. Coffa, G.A. Howe, A.R. Brash, Lipids 43 (2008) 979–987.
[97] S. Borngraber, M. Browner, S. Gillmor, C. Gerth, M. Anton, R. Fletterick, H. Kuhn, J. Biol. Chem. 274 (1999) 37345–37350.
[98] D.L. Sloane, R. Leung, J. Barnett, C.S. Craik, E. Sigal, Protein Eng. 8 (1995) 275–282.
[99] D.L. Sloane, R. Leung, C.S. Craik, E. Sigal, Nature 354 (1991) 149–152.
[100] S. Borngraber, R.J. Kuban, M. Anton, H. Kuhn, J. Mol. Biol. 264 (1996) 1145–1153.
[101] R. Vogel, C. Jansen, J. Roffeis, P. Reddanna, P. Forsell, H.E. Claesson, H. Kuhn, M. Walther, J. Biol. Chem. 285 (2010) 5369–5376.
[102] F. Burger, P. Krieg, F. Marks, G. Furstenberger, Biochem. J. 348 (Pt 2) (2000) 329–335.
[103] T. Watanabe, J.Z. Haeggstrom, Biochem. Biophys. Res. Commun. 192 (1993) 1023–1029.
[104] H. Suzuki, K. Kishimoto, T. Yoshimoto, S. Yamamoto, F. Kanai, Y. Ebina, A. Miyatake, T. Tanabe, Biochim. Biophys. Acta 1210 (1994) 308–316.
[105] K. Schwarz, M. Walther, M. Anton, C. Gerth, I. Feussner, H. Kuhn, J. Biol. Chem. 276 (2001) 773–779.
[106] E. Hornung, S. Rosahl, H. Kuhn, I. Feussner, Biochem. Soc. Trans. 28 (2000) 825–826.
[107] L. Toledo, L. Masgrau, J.D. Marechal, J.M. Lluch, A. Gonzalez-Lafont, J. Phys. Chem. B 114 (2010) 7037–7046.
[108] M. Jisaka, R.B. Kim, W.E. Boeglin, A.R. Brash, J. Biol. Chem. 275 (2000) 1287–1293.
[109] G.A. Veldink, G.J. Garssen, J.F. Vliegenthart, J. Boldingh, Biochem. Biophys. Res. Commun. 47 (1972) 22–26.
[110] E. Hornung, S. Kunze, A. Liavonchanka, G. Zimmermann, D. Kuhn, K. Fritsche, A. Renz, H. Kuhn, I. Feussner, Phytochemistry 69 (2008) 2774–2780.
[111] J.P. Falgueyret, D. Denis, D. Macdonald, J.H. Hutchinson, D. Riendeau, Biochemistry 34 (1995) 13603–13611.
[112] R. Mogul, E. Johansen, T.R. Holman, Biochemistry 39 (2000) 4801–4807.
[113] A.T. Wecksler, C. Jacquot, Biochemistry 48 (2009) 6259–6267.
[114] A.T. Wecksler, V. Kenyon, J.D. Deschamps, T.R. Holman, Biochemistry 47 (2008) 7364–7375.
[115] A.T. Wecksler, N.K. Garcia, T.R. Holman, Bioorg. Med. Chem. 17 (2009) 6534–6539.
[116] A.M. Aleem, J. Jankun, J.D. Dignam, M. Walther, H. Kuhn, D.I. Svergun, E. Skrzypczak-Jankun, J. Mol. Biol. 376 (2008) 193–209.
[117] E.H. Oliw, Prostaglandins Other Lipid Mediators 68–69 (2002) 313–323.
[118] L. De Petrocellis, V. Di Marzo, Prostaglandins Leukotrienes Essent. Fatty Acids 51 (1994) 215–229.
[119] D.J. Hawkins, A.R. Brash, J. Biol. Chem. 262 (1987) 7629–7634.
[120] H. Porta, M. Rocha-Sosa, Microbiology 147 (2001) 3199–3200.
[121] R.E. Vance, S. Hong, K. Gronert, C.N. Serhan, J.J. Mekalanos, Proc. Natl. Acad. Sci. USA 101 (2004) 2135–2139.
[122] T. Koeduka, T. Kajiwara, K. Matsui, Curr. Microbiol. 54 (2007) 315–319.
[123] M. Srivastava, E. Begovic, J. Chapman, N.H. Putnam, U. Hellsten, T. Kawashima, A. Kuo, T. Mitros, A. Salamov, M.L. Carpenter, A.Y. Signorovitch, M.A. Moreno, K. Kamm, J. Grimwood, J. Schmutz, H. Shapiro, I.V. Grigoriev, L.W. Buss, B. Schierwater, S.L. Dellaporta, D.S. Rokhsar, Nature 454 (2008) 955–960.
[124] G. Bannenberg, M. Martinez, M. Hamberg, C. Castresana, Lipids 44 (2009) 85–95.
[125] H. Toh, C. Yokoyama, T. Tanabe, T. Yoshimoto, S. Yamamoto, Prostaglandins 44 (1992) 291–315.
[126] J.H. Shin, K. Van, D.H. Kim, K.D. Kim, Y.E. Jang, B.S. Choi, M.Y. Kim, S.H. Lee, BMC Plant Biol. 8 (2008) 133.
[127] A.Z. Andreou, M. Vanko, L. Bezakova, I. Feussner, Phytochemistry 69 (2008) 1832–1837.
[128] I. Lang, I. Feussner, Phytochemistry 68 (2007) 1120–1127.

[129] I. Lang, C. Gobel, A. Porzel, I. Heilmann, I. Feussner, Biochem. J. 410 (2008) 347–357.
[130] A. Andreou, C. Gobel, M. Hamberg, I. Feussner, J. Biol. Chem. 285 (2010) 14178–14186.
[131] C. Mereschkowski, Biol Centralbl 25 (1905) 593–604.
[132] L. Sagan, J. Theor. Biol. 14 (1967) 255–274.
[133] C.Y. Huang, M.A. Ayliffe, J.N. Timmis, Nature 422 (2003) 72–76.
[134] P. Maliga, Nature 422 (2003) 31–32.
[135] C.Y. Huang, M.A. Ayliffe, J.N. Timmis, Proc. Natl. Acad. Sci. USA 101 (2004) 9710–9715.
[136] J.N. Timmis, M.A. Ayliffe, C.Y. Huang, W. Martin, Nat. Rev. Genet. 5 (2004) 123–135.
[137] W. Martin, B. Stoebe, V. Goremykin, S. Hapsmann, M. Hasegawa, K.V. Kowallik, Nature 393 (1998) 162–165.
[138] C. Barsan, P. Sanchez-Bel, C. Rombaldi, I. Egea, M. Rossignol, M. Kuntz, M. Zouine, A. Latche, M. Bouzayen, J.C. Pech, J. Exp. Bot. 61 (2010) 2413–2431.
[139] V.V. Emelyanov, Eur. J. Biochem. 270 (2003) 1599–1618.
[140] M. Johannesson, L. Backman, H.E. Claesson, P.K. Forsell, Prostaglandins Leukotrienes Essent. Fatty Acids 82 (2010) 121–129.
[141] T. Yoshimoto, H. Suzuki, S. Yamamoto, T. Takai, C. Yokoyama, T. Tanabe, Proc. Natl. Acad. Sci. USA 87 (1990) 2142–2146.
[142] X.S. Chen, U. Kurre, N.A. Jenkins, N.G. Copeland, C.D. Funk, J. Biol. Chem. 269 (1994) 13979–13987.
[143] T. Watanabe, J.F. Medina, J.Z. Haeggstrom, O. Radmark, B. Samuelsson, Eur. J. Biochem. 212 (1993) 605–612.
[144] M. Berger, K. Schwarz, H. Thiele, I. Reimann, A. Huth, S. Borngraber, H. Kuhn, B.J. Thiele, J. Mol. Biol. 278 (1998) 935–948.
[145] D. Sun, C.D. Funk, J. Biol. Chem. 271 (1996) 24055–24062.
[146] X.S. Chen, J.R. Sheller, E.N. Johnson, C.D. Funk, Nature 372 (1994) 179–182.
[147] E.N. Johnson, L.F. Brass, C.D. Funk, Proc. Natl. Acad. Sci. USA 95 (1998) 3100–3105.
[148] D. Poeckel, K.A. Zemski Berry, R.C. Murphy, C.D. Funk, J. Biol. Chem. 284 (2009) 21077–21089.
[149] H. Porta, M. Rocha-Sosa, Plant Physiol. 130 (2002) 15–21.
[150] I. Feussner, C. Wasternack, Annu. Rev. Plant Physiol. Plant Mol. Biol. 53 (2002) 275–297.
[151] B.A. Vick, D.C. Zimmerman, Biochem. Biophys. Res. Commun. 111 (1983) 470–477.
[152] I. Feussner, C. Wasternack, H. Kindl, H. Kuhn, Proc. Natl. Acad. Sci. USA 92 (1995) 11849–11853.
[153] J.F. Bousquet, K.V. Thimann, Proc. Natl. Acad. Sci. USA 81 (1984) 1724–1727.
[154] Y. He, H. Fukushige, D.F. Hildebrand, S. Gan, Plant Physiol. 128 (2002) 876–884.
[155] G. Chen, R. Hackett, D. Walker, A. Taylor, Z. Lin, D. Grierson, Plant Physiol. 136 (2004) 2641–2651.
[156] M. Ridolfi, S. Terenziani, M. Patumi, G. Fontanazza, J. Agric. Food Chem. 50 (2002) 835–839.
[157] W.C. Song, A.R. Brash, Arch. Biochem. Biophys. 290 (1991) 427–435.
[158] P. Aparoy, R.N. Reddy, L. Guruprasad, M.R. Reddy, P. Reddanna, J. Comput.-Aided Mol. Des. 22 (2008) 611–619.
[159] W. Humphrey, A. Dalke, K. Schulten, J. Mol. Graphics 14 (1996) 33–38.
[160] R.B. Russell, G.J. Barton, Proteins 14 (1992) 309–323.
[161] A. Varshney, F.P. Brooks, W.V. Wright, IEEE Comput. Graphics Appl. 14 (1994) 19–25.